Proc. NIPR Symp. Antarct. Meteorites, **6**, 364–373, 1993

Rb-Sr AGE OF AN IMPACT EVENT RECORDED IN YAMATO-791088 H CHONDRITE

Hirokazu FUJIMAKI[1], Ken-ichi ISHIKAWA[2], Hideyasu KOJIMA[3], Keizo YANAI[3] and Ken-ichiro AOKI[1]

[1] *Institute of Mineralogy, Petrology, and Economic Geology, Faculty of Science, Tohoku University, Aoba, Sendai 980*
[2] *College of General Education, Tohoku University, Aoba, Sendai 980*
[3] *National Institute of Polar Research, 9-10, Kaga 1-chome, Itabashi-ku, Tokyo 173*

Abstract: The age of the impact event is recorded in Yamato(Y)-791088, a high-iron type chondrite and has been dated using the Rb-Sr chronometer. A brief mineralogical characterization was made of the chondrite as well. The obtained impact age is 1024±47 Ma. When Y-791088 recorded the impact event, it might not have been on the surface of the parent body, but rather deep. Therefore, some sulfide was not vaporized and Rb was not lost during the impact. Metal phases were once homogenized and plessite, consisting of two phases, is really scarce. After the impact, the parental body could not have lasted long before separating into pieces.

1. Introduction

Some of the high-iron chondrites collected from Antarctica have recorded melting events presumably caused by asteroid impacts (YANAI and KOJIMA, 1987). The impact-melted, high-iron chondrites are, however, mostly small and the melting seems incomplete. Thus, none of the impact events of the high-iron chondrites from Antarctica have been successfully dated so far. Since the parent body was a whole object before the impact, the age of the impact-melting event indicates the minimum life span of the chondrite parent body (*e.g.*, NAKAMURA and OKANO, 1985; NAKAMURA *et al.*, 1990). Therefore, dating of the impact event is of vital importance to our understanding of the history of the parent planet. Yamato(Y)-791088 is a rather large, high-iron chondrite and a part of it seems to have been once molten. In this paper, we attempt to date the impact event recorded in the sample using the Rb-Sr chronometer. The mineralogical characteristics will be reported as well.

2. Sample

A small chip was cut from the Y-791088 chondrite (2.1 kg specimen) and 2.884 g was used for this experiment. The shock of the impact seems severe enough to have extensively deformed the shapes of the chondrules, but not strong enough to thoroughly erase them. Thus, the impact did not cause complete melting. Several chondrules are scarcely recognized within a 12 mm × 8 mm area of the thin section. Their shapes are

"pseudomorphs" of porphyritic chondrules, barred-olivine chondrules, and radial-pyroxene chondrules. The porphyritic chondrule includes rather large olivine and small rhombic pyroxene grains. In contrast, barred-olivine chondrules and radial pyroxene chondrules consist mostly of small crystals in cryptocrystalline materials. Large olivine and small rhombic pyroxene crystals exist in the matrix. Although most of the large olivine crystals show clear undulatory extinction, small ones do not. The matrix is a mixture of fine crystals and glasses with opaque minerals. Feldspar-like, skeletal, needle-like crystals were recognized in the mesostasis.

Metal is mostly homogeneous. Although H-type chondrites are usually dominated by kamacite (WOOD, 1967; NAGAHARA, 1979), the homogeneous metal phase is Ni-poor taenite. Ni-rich taenite is found only as exsolution lamellae in kamacite (plessite), although such plessite grains are few. Some of the metal grains are elongated and some are droplets. Iron sulfide is included in the sample, but much less abundant than the metal phase.

A number of vacant holes can be seen; some of them might have been formed during the making of the thin section, but others must be vesicles formed during the impact. Some holes are surrounded by yellow or brown alteration products and similar ones can be found all over the section. Metal or sulfide probably once filled some of the holes, but has since fallen out during thinning or polishing. Alteration seems so severe that yellow or brown, altered parts and holes occupy approximately 15% of the thin section area. Thus, we must be cautious when treating this sample for age dating, and the isotopic analysis of the whole rock sample is useless.

3. Experimental Method

Mineral compositions were determined with an electron microanalyzer at Tohoku University using similar methods reported elsewhere (FUJIMAKI and AOKI, 1982). The sample was crushed to below 100 mesh-size and separated into eight fractions in the same manner reported by FUJIMAKI *et al.* (1992). Some major elements were analyzed using a flameless atomic absorption spectrometer. Sr isotopic compositions were measured on a Finnigan MAT 261 solid-source mass spectrometer. Rb and Sr abundances were determined using the isotope dilution method. The chemical procedures, accuracy, and precision for the mass spectrometric analysis have been already described (FUJIMAKI *et al.*, 1992).

4. Mineral Compositions

Selected analytical results of silicate minerals and glasses in the sample are presented in Tables 1 and 2, respectively. Although grayish in color as a fine-grained material, similar to feldspar, Si-rich, Na-rich, and aluminous glasses are found in the mesostasis. All the analytical results of the minerals are plotted in Fig. 1.

Percentages of fayalite in olivine range from 18 to 21 mole%; a fairly narrow compositional range. Olivines are mostly small and abundant. One pseudmorphic, porphyritic chondrule includes large olivine crystals and a few crystal aggregates include large olivine crystals as well. Both large and small olivine crystals are in a similar

Table 1. Representative analytical results of olivine and pyroxene.

	R-ol1	R-ol2	I-ol1	I-ol2	L-px	Pg-1	Pg-2	Pg-3	Aug-1
SiO_2	38.96	38.71	39.27	39.06	56.66	56.17	54.65	54.28	53.91
TiO_2	—	—	—	—	0.07	0.05	0.11	0.16	0.32
Al_2O_3	—	—	—	—	0.19	1.55	1.76	3.15	4.38
Cr_2O_3	0.34	0.32	0.43	0.75	0.04	0.50	0.69	0.89	1.25
FeO	16.79	16.91	18.60	18.03	11.70	10.66	10.82	10.82	8.47
MnO	0.47	0.43	0.56	0.45	0.45	0.45	0.55	0.40	0.34
MgO	42.55	42.55	41.43	42.10	30.65	26.10	23.07	23.32	17.60
CaO	0.10	0.10	0.21	0.18	0.73	3.94	7.52	6.30	12.04
Na_2O	—	—	—	—	—	0.57	0.68	1.22	1.42
Total	99.21	99.02	100.50	100.57	100.49	99.99	99.85	100.54	99.73
Fa	18.5	18.6	20.6	19.8					
Fs					17.9	17.7	18.3	18.4	16.8
Wo					1.4	8.0	15.5	13.3	34.0

R-ol1: large olivine in porphyritic chondrule, R-ol2: large olivine in matrix, I-ol1: small olivine in a chondrule, I-ol2: small olivine in matrix, L-px: large Ca-poor pyroxene (orthopyroxene), Pg-1 to Pg-3: pigeonite, Aug-1: Ca-rich pyroxene (augite), Fa: fayalite, Fs: ferrosilite, Wo: wollastonite, —: not detected.

Table 2. Representative analytical results of glass.

	1	2	3	4
SiO_2	62.79	62.11	66.89	65.27
TiO_2	0.37	0.37	0.46	0.01
Al_2O_3	17.79	17.40	19.86	22.08
Cr_2O_3	0.06	—	—	—
FeO	3.94	4.92	1.73	3.62
MnO	0.04	0.03	—	0.10
MgO	2.85	4.83	1.06	1.44
NiO	—	0.31	—	—
CaO	1.89	2.12	2.33	1.89
Na_2O	8.13	7.87	6.03	4.58
K_2O	—	0.03	1.65	0.99
S	2.14	—	—	—

Total is calculated to 100%. —: not detected.

compositional range regardless of where they are found. All olivines include Cr, but its valence is not known. Although Cr is possibly divalent in olivine, the trivalent state was used to express its weight percent and cation formula. They have nearly no Ni. The CaO contents in large olivines are mostly 0.1 wt%, while those in small olivines are more than 0.15 wt%. The CaO contents are similar to those of the igneous olivines in the Shaw meteorite (TAYLOR *et al.*, 1979).

No Ca-poor clinopyroxene was found. All the Ca-poor pyroxenes whose sizes were identifiable under the microscope were rhombic. Orthopyroxenes are within the composition of bronzite and their enstatite component ranges from 17% to 20%. Some of them are rather rich in Ca and some in Al. Their Mg/(Mg+Fe) ratio is limited,

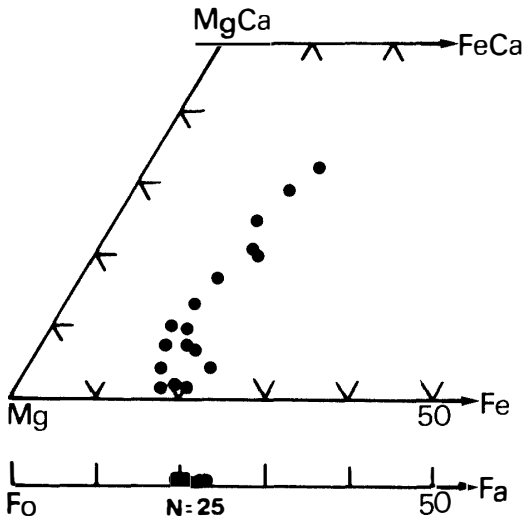

Fig. 1. Chemical compositions of olivines and pyroxenes in Y-791088 H chondrite.

Table 3. Representative analytical results of metal and troilite.

	1	2	3	4	Troilite
Fe	93.18	92.30	91.04	91.38	64.41
Ni	6.62	7.89	9.17	9.26	n.d.
S	—	—	—	—	36.69
Total	99.80	100.19	100.21	100.64	100.10
Atomic %					
Fe	93.7	92.5	91.3	91.2	50.2
Ni	6.3	7.5	8.7	8.8	
S					49.8

1–2: Kamacite, 3–4: Ni-poor taenite, n.d.: not detected.

while the Al content varies to some extent. The highly-deformed, radial-pyroxene chondrule includes a number of pyroxene crystals. The Al and Ca contents of the small orthopyroxenes in a single relict chondrule are variable. Pigeonitic pyroxenes and tiny subcalcic augite coexist with orthopyroxenes in both the chondrule and in the matrix. They have variable Ca contents with narrow Mg/(Mg + Fe) ratios (Fig. 1). The chemical variation of the pyroxenes is rather similar to that of Yamato-790964 LL chondrite reported by MIYAMOTO *et al.* (1984), although the Mg/(Mg + Fe) ratios differ between the two chondrites. Although some of the analytical results implied the possible existence of diopsidic pyroxene, none of them fit perfectly with the pyroxene formula. Thus, they were not tabulated.

The sums of the analytical results of glasses are usually less than 97%, so the results were normalized to 100%. The glasses are highly enriched in Al and Na. The Al contents in the glasses are reversely correlated with the Na contents. Some contain S and some Ni.

The representative analytical results of metal phases and troilite are shown in Table 3. Metals in common H-type chondrites are dominated by kamacite and taenite

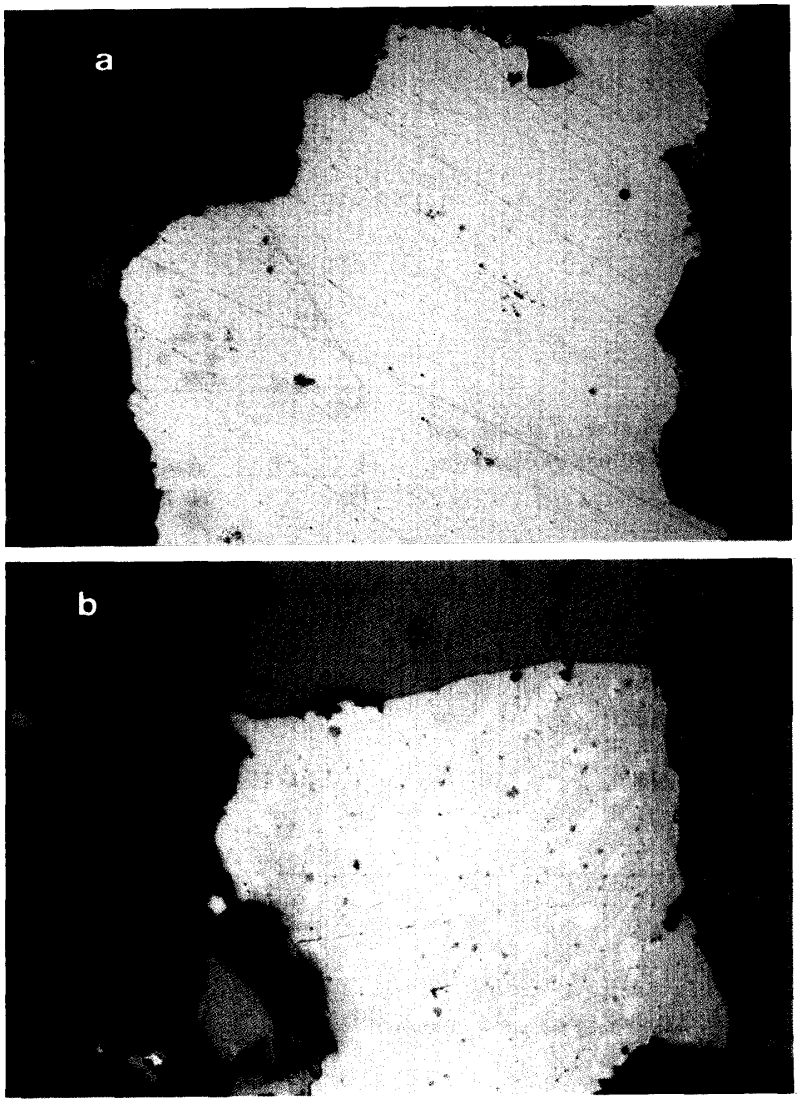

Fig. 2. (a) Photomicrograph of homogeneous Ni-taenite. Reflected light. Horizontal length of the photo is approximately 0.12 mm. (b) Photomicrograph of kamacite (plessite) including Ni-rich taenite globules. Note taenite is light white in dark white kamacite. Reflected light. Horizontal length of the photo is approximately 0.05 mm. S: sulfide (troilite).

associates. In contrast, the metal phases in Y-791088 are more than 7 wt% Ni, but less than 9 wt%. Kamacite is unlikely: the compositions are in the middle of the miscibility gap of the Fe-Ni binary phase relation (GOLDSTEIN and OGILVIE, 1965; MOREN and GOLDSTEIN, 1978; WILLIS and WASSON, 1978). The metal phases in Y-791088 are homogeneous in Fig. 2a; readers may note that there are no microscopic exsolutions in the metal, and they are hardly recognized in most of the metals at all. A few of them include very fine exsolution lamellae as shown in Fig. 2b. They are globule-like lamellae of taenite in kamacite (plessite). This kind of exsolution is very rare in Y-791088. The frequency diagram of weight percent Ni in the metals is shown in Fig. 3. In comparison with a similar figure reported by NAGAHARA (1979), the Ni enrichment in the metal

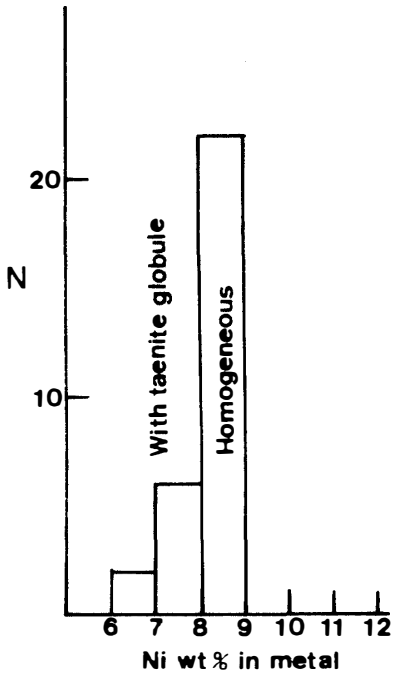

Fig. 3. Frequency diagram of Ni content in metal phases of Y-791088.

phases in Y-791088 can be recognized. Since most of the metal phases plot in the middle of the solvus at temperatures below 700°C, they are probably taenite quenched at high temperature. Exsolved taenite could not be analyzed because of its fine-grained size.

Only one analytical result of troilite is shown in Table 3. Although we analyzed a number of troilite grains in the sample, troilite in Y-791088 does not contain measurable amounts of Ni when using an electron microanalyzer. Most of the analytical results do not fit to the stoichiometric formula of troilite, and S is always deficient. Thus, most of the sulfides may not be troilite, but some kind of pyrrhotite. Some sulfides are associated with metals, but some are not. It is important to state that most impact-melted, L-type and LL-type chondrites scarcely contain sulfide.

5. Compositions of the Fractions

We separated the chondrite into eight fractions using their magnetic susceptibilities. The constituents were examined by X-ray diffraction. The two most magnetic fractions (M1 and M2) are dominated by metal, olivine, and pyroxenes, and nearly no glass. The other fractions contain both silicate minerals and glasses, but nearly no metal. We attempted to separate the sample into diversified glasses and not into mineral phases. Reddish-white alteration products were concentrated in the least magnetic fraction (M8). The analytical results of some of the major elements are shown in Table 4. The analysis was made on eluted solutions from the ion exchange columns. The iron contents were calculated as metallic Fe in the first two fractions. FeO was used to express the iron contents in the other fractions. Small but clear differences in the CaO and Na_2O contents can be noted among them, and similar variations would be expected in Rb abundances and corresponding Sr isotopic compositions. The two most magnetic fractions are highly enriched in Fe. Some silicate phases and glasses are included in

Table 4. Weight and partial analyses of the fractions.

	Weight (mg)	MgO	CaO	Fe*	FeO**	MnO	Na_2O	K_2O
M1	581	3.02	0.29	83.56		0.05	1.81	0.06
M2	422	7.66	0.70	62.96		0.13	0.76	0.12
M3	428	22.34	1.79		22.34	0.34	1.13	0.17
M4	187	25.18	1.98		17.30	0.35	1.22	0.14
M5	91	23.55	1.84		13.70	0.32	1.67	0.11
M6	76	26.59	2.02		14.81	0.39	1.40	0.15
M7	78	28.73	2.12		13.86	0.38	1.86	0.11
M8	891	26.31	1.60		13.62	0.55	1.71	0.10

M1 is the most magnetic fraction, and M8 is the least magentic or non-magnetic fraction. * and **: Iron content is expressed as metallic Fe for the two highly magnetic fractions, and FeO for the other fractions.

these two fractions since perfect separations were not attempted. Sulfide (troilite) is included in the less magnetic fractions, but its amount is very small. The FeO content decreases from the third magnetic fraction (28.7%) to the fifth magnetic fraction (17.6%). This tendency is consistent with the decrease in magnetic susceptibility. No obvious tendency between the FeO contents and their magnetic properties is recognized for the less magnetic fractions. Although the sample was carefully leached before crushing, a number of alteration products remained in the sample. Some alteration products tend to be associated with the metal phase. If they were not detached from the metal grains during crushing, they are included in the highly magnetic fractions. Many vesicles are surrounded by alteration products as well. This kind of dissociated product is included in the least magnetic fraction (M8 in Table 4). Therefore, the two most magnetic fractions as well as the least magnetic fraction should be considered questionable, and their results excluded from the isochron calculation.

6. Rb-Sr Age of the Impact Event

The Rb, Sr abundances, calculated $^{87}Rb/^{86}Sr$ ratios, and Sr isotopic compositions are given in Table 5. The two most magnetic fractions are poor in both Rb and Sr. The other fractions are not very enriched in Rb either. The range of $^{87}Rb/^{86}Sr$ values range from 0.3443 to 0.6023, excluding the M1, M2, and M8 fractions. No clear correlation is recognized between their magnetic susceptibility and their $^{87}Rb/^{86}Sr$ ratios. It should be pointed out that a sort of correlation exists between K_2O and Rb abundances among the five fractions.

All the isotopic results are plotted in Fig. 4. Excluding the two most magnetic fractions and the least magnetic fraction, the remaining five fractions appear to form a line. The calculated age is 1024 ± 47 Ma (2σ) with an initial ratio of 0.7240 (2σ). Estimated analytical errors are 0.4% for $^{87}Rb/^{86}Sr$ ratio and 0.008% for $^{87}Sr/^{86}Sr$ (1σ). The calculation uses the method proposed by YORK (1969) and the decay constant is from STEIGER and JÄGER (1977). This obtained age is the youngest one for an impact event on a high-iron chondrite. Thus, the H chondrite parent body was still

Table 5. Rb and Sr concentrations and $^{87}Sr/^{86}Sr$ ratios of the fractions.

	Rb	Sr	$^{87}Rb/^{86}Sr$	$^{87}Sr/^{86}Sr$	$2\sigma_{mean}$
M1	0.314	2.71	0.3352	0.713891	±0.000018
M2	1.06	5.95	0.5162	0.724707	±0.000020
M3	2.46	14.2	0.5035	0.731508	±0.000016
M4	2.54	13.9	0.5319	0.732044	±0.000017
M5	2.15	12.1	0.5157	0.731470	±0.000020
M6	2.88	24.3	0.3443	0.729051	±0.000014
M7	1.95	9.39	0.6023	0.732748	±0.000021
M8	2.49	12.3	0.5862	0.741482	±0.000021

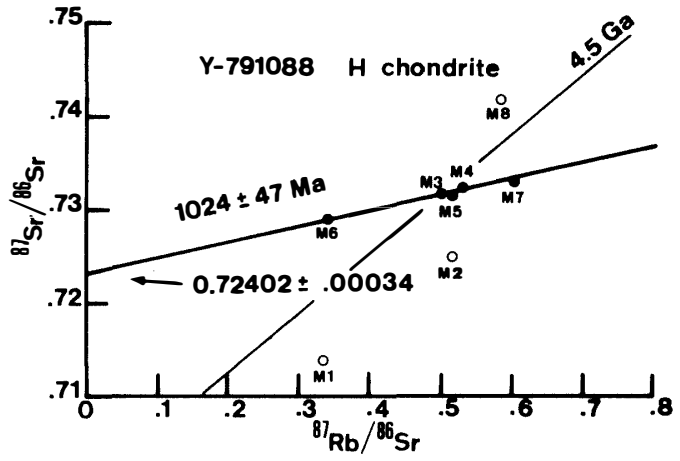

Fig. 4. Calculated isochron of the impact event recorded in Y-791088. Solid circles: M3 to M7, Open circles: M1, M2 and M8 (not used in the calculation). 4.5 Ga reference line is shown. The uncertainty associated with the age calculation is expressed as 2σ.

complete approximately 1 Ga ago. A 4.5 Ga reference line is drawn for comparison. Although we did not calculate the bulk or whole-rock datum, it should be very close to the 4.5 Ga isochron since the 4.5 Ga isochron passes through in the middle of our data. The bulk isotopic data of the impact-melted, low-iron chondrites usually plot on the left or upper side of the 4.5 Ga-isochron, usually, due to Rb loss (*e.g.*, MINSTER and ALLÈGRE, 1979b, 1981).

The M1 and M2 fractions plot on the right and M8 on the left of the 4.5 Ga reference line. The M1 and M2 appear to contain excess Rb and M8 seems to be deficient in Rb. They are somewhere between the 1 Ga isochron and the 4.5 Ga reference line before alteration since they are mixtures. Although we cannot approximate how much Rb and Sr they had before the alteration, at least redistribution of Rb can be considered among the altered phases. Assuming that the M8 fraction lost Rb, and the M1 and M2 fractions acquired it, the excess Rb of M1 and M2 as well as Rb deficiency of M8 can be accounted for.

7. Where was Y-791088 in the Parent Body?

Let us summarize several significant points:

(1) mafic minerals have rather homogeneous Mg/(Mg+Fe) ratios,
(2) most metals are Ni-poor taenites,
(3) plessite is exceedingly rare,
(4) sulfide remains, and
(5) Rb-loss is negligible.

Complete melting of Y-791088 is unlikely as evidenced by pseudomorphic chondrules. The existence of sulfide and lack of Rb loss may possibly imply that the impact was weak. However, pigeonite geothermometry gave equilibration temperatures as high as 1170 to 1190°C (ISHII, 1975). This high temperature must have been achieved by severe shock during the impact, the temperatures high enough to homogenize the metal phases. The high temperatures, however, conflict with the presence of sulfide and lack of Rb loss.

If Y-791088 was on the surface of the parent body when it was impacted, S would have been vaporized and considerable amounts of Rb and other volatile elements would have been lost. However, if Y-791088 was situated deep within the parent body of 150–175-km radius (MINSTER and ALLÈGRE, 1979a), S could have been retained in sulfide minerals and Rb would not have been lost due to confining pressures. A similar lack of Rb loss was also reported for the shock-melted Yamato-79 LL-chondrites (OKANO *et al.*, 1990). The constituent silicate minerals could be thermally homogenized *in situ* within the parent body. In contrast, the metal phase should have exsolved taenite lamellae in the kamacite host before the impact, which melted the metals into homogeneous phases again. They were subsequently not thermally metamorphosed for long, since plessite is rare and many of the metals are still homogeneous. This scenario can account for the observed mineralogical and geochemical characteristics. Accordingly, we prefer the idea that Y-791088 was deep within the parent body when impacted and was then already thermally metamorphosed. We have no idea how deep. The metal phases do give us some clues to approach this issue. The remaining homogeneous metals and a few exsolved ones imply that Y-791088 was not too deep in order to keep temperatures high for long, but not too shallow to be quenched right after the impact. Also, mineralogical features of the metals provide significant implications. No plessite can be formed without a long-term thermal metamorphism after homogenization during impact-induced heating. The scarcity of plessite, therefore, indicates that the total collision of the H chondrite parent body might have occurred sometime after 1 Ga, and fragmentation not long after 1 Ga.

8. Conclusion

Y-791088 was impacted 1024 Ma. When it was impacted, Y-791088 was heated up higher than 1100°C at depth within the parent body. The depth cannot be estimated accurately but it was deep enough not to vaporize S and Rb. Therefore, the presence of sulfide and lack of Rb loss was due to the confining pressure. The silicate minerals were thermally homogenized before the impact. The parent body might have fragmented

sometime after this impact, because plessite is exceedingly rare in Y-791088.

Acknowledgments

We are grateful to NIPR for giving us a great opportunity and financial support to study Y-791088. We also thank all the colleagues of the laboratory for helping us in the experiments. This study was partly supported by Grant-in-Aid (#02453045 to K. AOKI) for Scientific Research from Ministry of Education, Science and Culture of Japan.

References

FUJIMAKI, H. and AOKI, K. (1980): Quantitative microanalyses of silicates, oxides and sulfides using an energy-dispersive type electron probe. Sci. Rep. Tohoku Univ., Ser. III, **14**, 261–268.

FUJIMAKI, H., ISHIKAWA, K. and AOKI, K. (1992): Rb-Sr features of the impact-melted LL-chondrites from Antarctica: Yamato-790723 and Yamato-790528. Proc. NIPR Symp. Antarct. Meteorites, **5**, 290–297.

GOLDSTEIN, J. I. and OGILVIE, R. E. (1965): The growth of the Widmanstätten pattern in metallic meteorites. Geochim. Cosmochim. Acta, **29**, 893–920.

ISHII, T. (1974): The relations between temperature and composition of pigeonite in some lavas and their application to geothermometry. Mineral. J., **8**, 48–57.

MINSTER, J. F. and ALLÈGRE, C. J. (1979a): ^{87}Rb–^{87}Sr chronology of H chondrites: Constraint and speculations on the early evolution of their parent body. Earth Planet. Sci. Lett., **42**, 333–347.

MINSTER, J. F. and ALLÈGRE, C. J. (1979b): ^{87}Rb–^{87}Sr dating of L chondrites: Effects of shock and brecciation. Meteoritics, **14**, 235–248.

MINSTER, J. F. and ALLÈGRE, C. J. (1981): ^{87}Rb–^{87}Sr dating of LL chondrites. Earth Planet. Sci. Lett., **56**, 89–106.

MOREN, A. E. and GOLDSTEIN, J. I. (1978): Cooling rate variations of group IVA iron meteorites. Earth Planet. Sci. Lett., **40**, 151–161.

NAGAHARA, H. (1979): Petrological study of Ni-Fe metal in some ordinary chondrites. Mem. Natl Inst. Polar Res., Spec. Issue, **15**, 111–122.

NAKAMURA, N. and OKANO, O. (1985): 1,200-Myr impact-melting age and trace-element chemical features of the Yamato-790964 chondrite. Nature, **315**, 563–566.

NAKAMURA, N., FUJIWARA, T. and NOHDA, S. (1990): Young asteroid melting event indicated by Rb-Sr dating of the Points of Rocks meteorite. Nature, **345**, 51–52.

OKANO, O., NAKAMURA, N. and NAGAO, K. (1990): Thermal history of the shock-melted Antarctic LL-chondrites from the Yamato-79 collection. Geochim. Cosmochim. Acta, **54**, 3509–3523.

STEIGER, R. H. and JÄGER, E. (1977): Subcommission on geochronology: Convention on the use of decay constants in geo- and cosmochronology. Earth Planet. Sci. Lett., **36**, 359–362.

TAYLOR, G. J., KEIL, K., BERKLEY, J. L., LANGE, D. E., FODOR, R. V. and FRULAND, R. M. (1979): The Shaw meteorite: History of a chondrite consisting of impact-melted and metamorphic lithologies. Geochim. Cosmochim. Acta, **43**, 323–337.

WILLIS, J. and WASSON, J. (1978): Cooling rates of group IVA iron meteorites. Earth Planet. Sci. Lett., **40**, 141–150,

WOOD, J. A. (1967): Chondrites: Their metallic minerals, thermal histories, and parent planet. Icarus, **6**, 1–49.

YANAI, K. and KOJIMA, H., comp. (1987): Photographic Catalog of the Antarctic Meteorites. Tokyo, Natl Inst. Polar Res., 298 p.

YORK, D. (1969): Least-squares fitting of a straight line with correlated errors. Earth Planet. Sci. Lett., **5**, 320–324.

(Received October 29, 1992; Revised manuscript received January 5, 1993)